Aalborg Universitet

Efficiency and reliability improvement in wind turbine converters by grid converter adaptive control

Trintis, Ionut; Munk-Nielsen, Stig; Abrahamsen, Flemming ; Thøgersen, Paul Bach

Efficiency and Reliability Improvement in Wind Turbine Converters by Grid Converter Adaptive Control

Ionut Trintis [1], Stig Munk-Nielsen [1], Flemming Abrahamsen [2], Paul Bach Thoegersen [2]

[1] Department of Energy Technology
Aalborg University
Pontoppidanstraede 101
DK-9220, Aalborg, Denmark
Email: itr@et.aau.dk
URL: http://www.et.aau.dk

[2] KK-Electronic A/S
Boegildvej 3
DK-7430 Ikast, Denmark
URL: http://www.kk-electronic.com

Acknowledgments

Keywords

<<Converter control>>, <<Efficiency>>, <<Reliability>>, <<Adaptive control>>.

Abstract

This paper presents a control method that reduces the losses in wind turbine converters adaptively controlling the grid converter. The dc-link voltage adapts its reference based on the system state and therefore reduces the stored energy, and is therefore kept at the minimum necessary for the grid and generator side. Operating in this way, the electrical and thermal stress factors are decreased on the power electronic devices, increasing their lifetime. The simulation results using this method show efficiency increase and devices temperature cycles slightly decreased. Experimental results on a wind turbine power stack shows efficiency increase in the high power region.

Introduction

Wind turbines are emerging energy sources in the power grid, with exponential installed capacity over the past years. The output power of a single turbine has also increased over the years, now being in the MW range [1],[2]. Induction generator was at the ground of the wind turbines development, and the synchronous generators are gaining significant attention in recent years due to their advantages. For most of the generator technologies, the controllability and power processing is realized with a back to back converter. The efficiency and reliability of the wind turbine converter are very important for the entire system, and new ways to improve these factors are always welcome [3].

The generator is decoupled from the grid in the dc-link of the wind turbine converter, as seen in Figure 1. The grid converter is the component that controls the voltage level of the dc-link in order to maintain the energy balance between the two power sources, generator and grid. One way to reduce the stress on the

power electronic devices, from a back to back converter, is to reduce the operating dc-link voltage to a minimum.
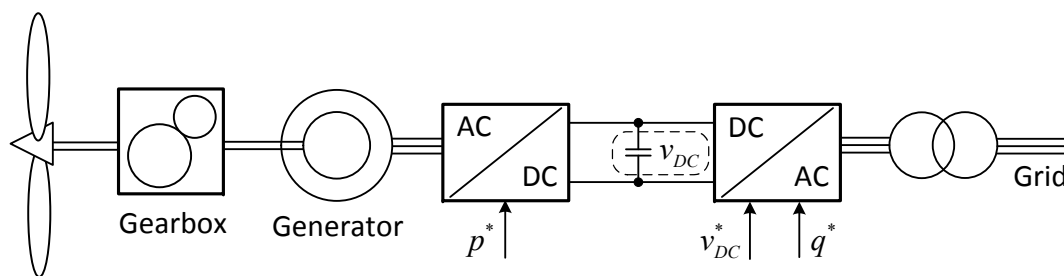

Figure 1: Wind Turbine System with Full Scale Converter

The general state-of-the-art control structure of the grid converter is shown in Figure 2. The converter synchronizes with the grid voltage, and controls the grid currents according to the references given to the current controller. The active current reference is given by the dc-link voltage controller, and can be also influenced by the frequency control. The dc-link voltage control dynamics can be improved with a feed-forward from the generator control, to allow fast power ramps.
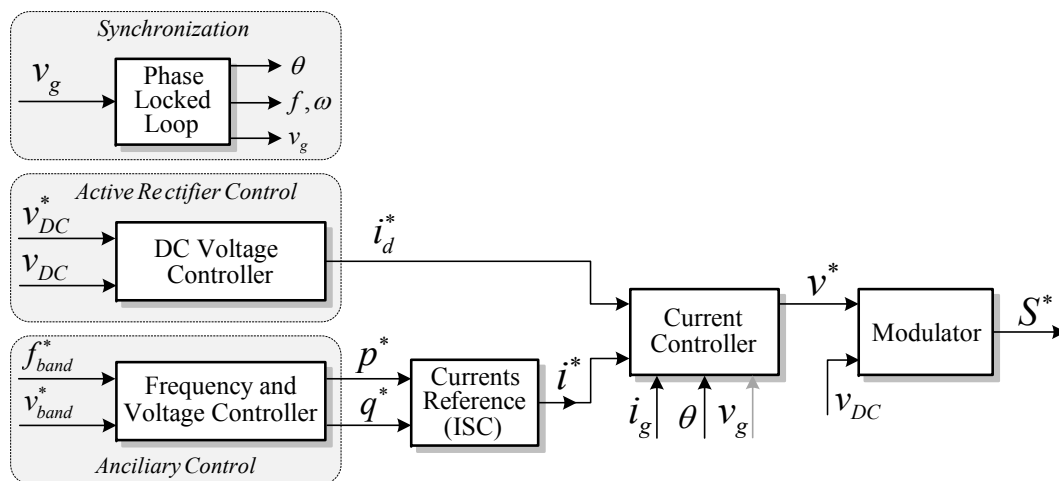

Figure 2: State of the Art Wind Turbine Grid Converter Control

Normally the dc-link voltage reference is fixed, and setup to a level that allows the converter operation over the entire power range and can achieve certain dynamics of the current controller. Reducing the energy stored in the dc-ink can bring benefits in efficiency and reliability of both the grid and the generator converters.

A method that calculates an offline table for the dc-link voltage, based on the operation of both grid and generator converters was introduced in [4]. It was also shown that the reliability can be increased due to the reduced failure rate based on cosmic rays. This method is however dependent on the model of the grid and generator, which include parameters that can change depending on various factors like operating temperature of the generator, grid overvoltage, grid impedance and LCL filter impedance.

Adaptively adjusting the dc-link voltage reference online can eliminate the calculation errors based on the involved systems modelling.

This paper proposes an additional control loop as outer loop to the dc-link voltage controller, which adapts the voltage reference with regard to the system state. The dc-link voltage reference is therefore online calculated to the minimum necessary for operating the generator and grid converters. It is proven by simulation of a 6 MW wind turbine grid converter that a slight increase in efficiency and decrease of the thermal stress on power devices. Experimental results of a wind turbine power stack prove the efficiency increase in the high power region.

Adaptive DC Voltage Control

A low bandwidth controller that is to be used as outer loop of the current and dc-link voltage control loops of the wind turbine's grid converter is described in the followings. To achieve an online adaptation of the dc-link voltage reference, a control loop can be implemented as shown in Figure 3. Instead of setting only the dc-link voltage reference, the maximum modulation index reference is controlled taking the feedback from the input modulation index to the modulators. Thus, the dc-link voltage is indirectly adapted by the maximum modulation index reference, but also depending on the state of the grid, generator, and the operating point.
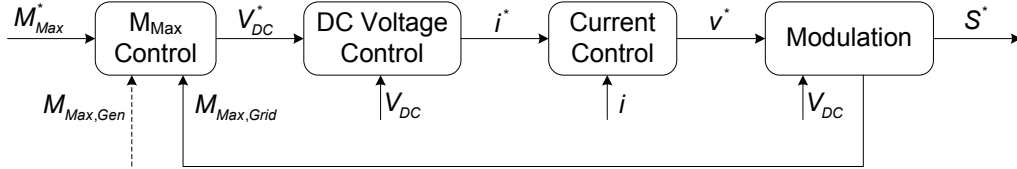

Figure 3: Proposed adaptive dc-link voltage controller

The single phase equivalent circuit of the generator to grid is shown in Figure 4. Here, v_G is the internal generator voltage, i_G and z_G are the generator current and impedance at the given operating point of the wind turbine. Respectively v_g, i_g and z_g are the grid voltage, current and impedance at the given operating point.
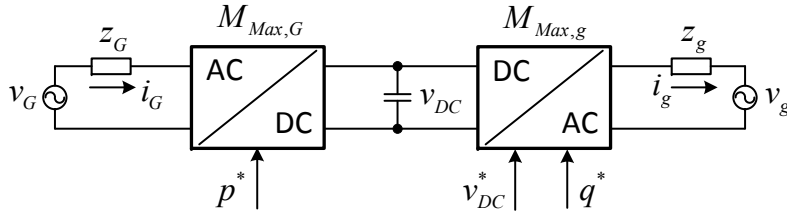

Figure 4: Basic equivalent electrical circuit of the wind turbine

Disregarding the associated losses, the converter output voltage generalized for either grid or generator side is given by:

$$v_c = \frac{v_{DC}}{2} \cdot \left(1 + \frac{2}{\sqrt{3}} \cdot M_{Max,c} \cdot (sin(\theta_c) - v_{3h,c}(\theta_c))\right) \tag{1}$$

Here, v_{DC} is the actual dc-link voltage, $M_{Max,c}$ is the maximum modulation index, θ_c is the control angle and $v_{3h,c}$ is the third harmonic offset voltage, all for the converter "$_c$". The third harmonic offset voltage $v_{3h,c}$ is dependent on the chosen modulation technique, resulting continuous or discontinuous pulse width modulations [5].

Considering the equivalent circuit from Figure 4, and using (1) for both grid and generator converters, the maximum modulation index is given by:

$$M_{Max,g} = \frac{v_g(t) + i_g(t) \cdot R_g + L_g \cdot \frac{di_g}{dt} - \frac{v_{DC}}{2}}{\frac{v_{DC}}{\sqrt{3}} \cdot (sin(\omega t) + v_{3h,g}(t) - v_{nh,g}(t))} \tag{2}$$

$$M_{Max,G} = \frac{v_G(t) - i_G(t) \cdot R_G - L_G \cdot \frac{di_G}{dt} - \frac{v_{DC}}{2}}{\frac{v_{DC}}{\sqrt{3}} \cdot (sin(\omega t) + v_{3h,G}(t))} \tag{3}$$

In (2) the maximum modulation index is given for the grid side converter, where the additional voltage $v_{nh,g}$ is the additional harmonic voltage produced by the converter to compensate the grid harmonics. The $M_{Max,g}$ is basically influenced by the voltage that the converter produces to inject the desired current

i_g. Thus, $M_{Max,g}$ is direct proportional with the grid voltage, current, impedance and additional harmonic voltage respectively and inverse proportional with the dc-link voltage v_{DC}.

In (3) the maximum modulation index is given for the generator side converter $M_{Max,G}$. On the generator side, considering ideal dc-link decoupling from the grid, the $M_{Max,G}$ is direct proportional with the generator internal voltage and inverse proportional with the generator current, generator impedance and with the dc-link voltage. It must be noted that the maximum modulation index depends also on the power factor, because the currents i_g and i_G are complex numbers including reactive currents as well.

Online Maximum Modulation Index Detection

As can be seen from equations (2) and (3), a reduction of the dc-link voltage can only be done by online monitoring of the maximum modulation index of both the grid and generator converter, because it depends on many parameters. The grid state, generator state, or even the converter hardware can influence the maximum modulation index. Therefore, it is strictly necessary to online monitor this parameter of both converters grid and generator, and adapt the dc-link voltage accordingly using the grid converter, when the dc-link voltage utilisation is optimized.

The online detection of the modulation index can be implemented with different update rates, depending on how many sectors are monitored in one cycle. The space vector modulation sectors are shown in Figure 5, with the fundamental frequency components in the right side.
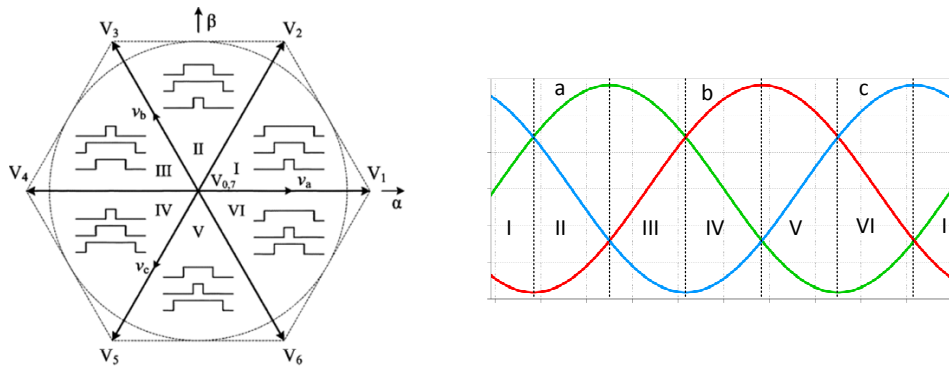

Figure 5: Space vector modulation sectors

A maximum and minimum is present in each sector, therefore the maximum update rate can be implemented each 60 degrees. The maximum modulation index each 60 degrees is however depending on one phase at a time, and each 120 degrees it will be detected the maximum of one of the three phases. The difference between phases can therefore generate harmonic ripple on the feedback signal, effect which must be dealt with in the control scheme.

The simplest approach is to monitor the maximum each fundamental period. In this case, the update rate is the slowest but the maximum modulation index feedback contains the maximum of all three phases. The unwanted harmonic ripple on feedback is eliminated at the sacrifice of increased control delay. Therefore, when tuning the M_{Max} control loop the delay generated by the detection algorithm has to be considered.

A maximum modulation index reference is given instead, and the output dc-link voltage reference will adapt to the entire system state. The feedback is detected from both the grid and generator converters modulators, and the maximum index of both will be regulated by the M_{Max} control loop.

In this way the operating dc-link voltage is reduced significantly at all power levels, and more consistently at light load. Ideally the maximum modulation index reference should be as high as possible for the grid converter, but a reserve should be kept to allow operation not only in steady state, also with slow changes in power for a given maximum dP/dt. Physical limitations like the dead time and minimum pulse width effects will reduce the practical maximum reference.

Simulation Results

To demonstrate the operation of the proposed controller, a simulation model was implemented in PLECS. The detailed control structure is shown in Figure 6. The input to the control structure is the maximum modulation index reference and taking the feedback from the modulator, the error is regulated by the modulation index controller. This case assumes that the wind turbine generator rated voltage is smaller as compared with the grid voltage, and therefore the modulation index of the generator converter is always smaller compared with the grid converter.

The output of the M_{Max} controller is an adjustment δV_{DC} of the reference dc-link voltage added to a feedforward therm V_{DC}^* based on the grid parameters. The resulting dc-link voltage reference is regulated by the DC voltage controller having the measured dc-link voltage V_{DC} as feedback. Proportional integral (PI) controllers are used for all control loops. The current control is realized in a standard decoupled dq rotating reference frame [6],[7].
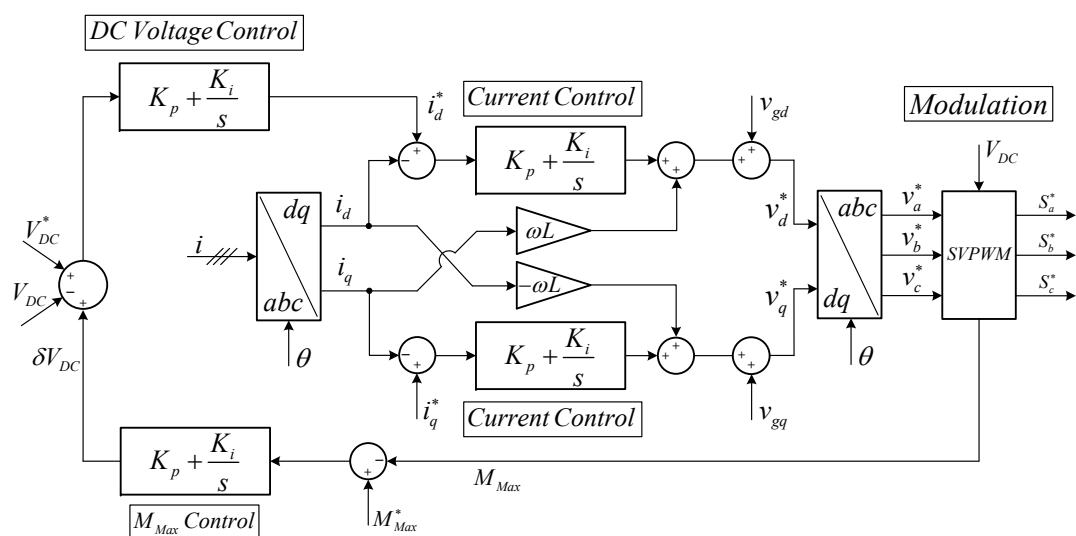

Figure 6: Grid converter *dq* adaptive control structure

The converter topology considered in simulation is the classical two level converter connected to a low voltage 690 V transformer, using six 1700 V and 1400 A IGBT modules in parallel for each switch (Infineon FF1400R17). The model of the output L filter and grid impedances was assumed to be 70 mH and 2 mΩ in total, and the total installed dc-link capacitance was 10 mF. The rated power was 6 MW, with devices maximum junction temperature of 150 °C.

The controller operation is shown in Figure 7, enabled at 1.5 s with converter operating in steady state at 50% of the rated power. The maximum modulation index reference in this case was set to 0.999. Continuous space vector modulation was applied in this case, with 4 μs deadtime and without using a minimum pulse width filter. After enabling the controller the detected modulation index is increased and controlled to the reference value with a time constant of 1 s. The operating dc-link voltage is therefore reduced to around 1000 V, with 50 V less as compared with the fixed reference (1050 V) that is normally set for all operating points.

A thermal model was included, calculating losses using look up tables with datasheet information [8],[9]. The heatsink temperature was set to 80 °C. In Figure 7 can also be seen the temperature of a high side transistor and its freewheeling diode. It can be noticed a slight reduce of the average operating temperature and the temperature cycle of the devices due to a reduced power loss in steady state of the proposed controller at 2.5 s. The maximum IGBT junction temperature decreases from 109.3 °C to 108.5 °C, and the temperature cycle ΔT from 11.2 °C down to 10.9 °C for the previously described operating condition. For diode the maximum junction temperature decreases from 96.1 °C down to 95 °C, and the ΔT from 6.7 °C down to 6.3 °C.

Due to reduced operating dc-link voltage, also the ripple current on the output L filter is reduced. Figure 8
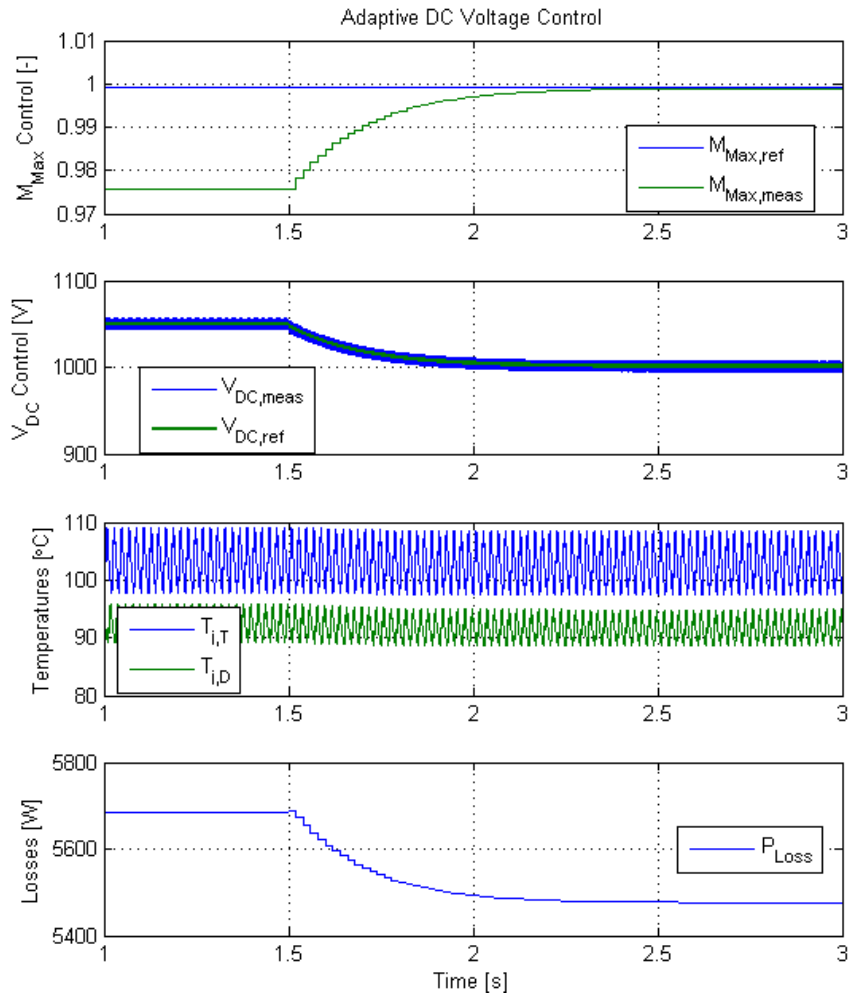
Figure 7: Controller operation at 50% load (3 MW)

shows the results for the semiconductor efficiency and Figure 9 shows the total harmonic distortion using a fixed reference dc-link voltage and adaptive dc-link voltage control of the grid converter. It can be noticed improvement in both efficiency and output harmonic distortion, and more consistent for light load operation. The wind turbine power savings are calculated only in the grid converter, and at least similar efficiency improvement is expected also for the generator side converter.
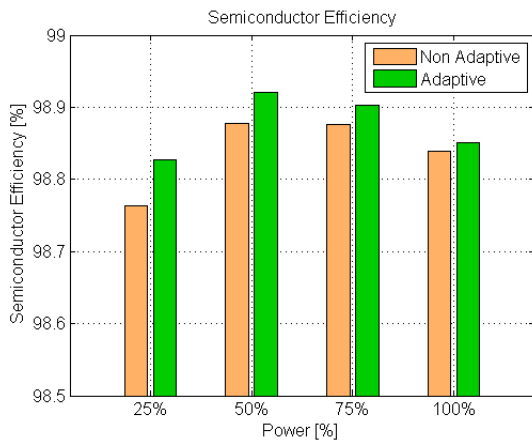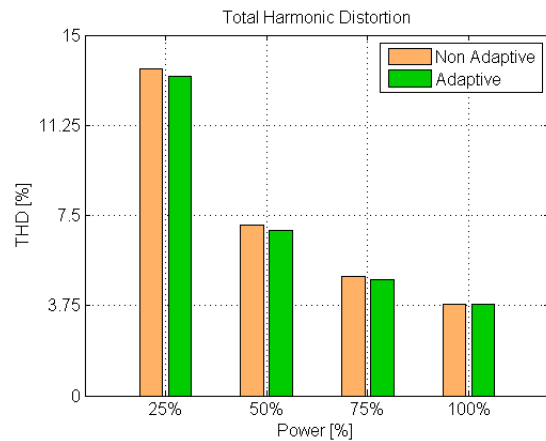

Figure 8: Efficiency

Figure 9: THD

The non-linear effect of the minimum pulse width filter must also be considered when weighting the

THD of the two operating modes. For high modulation indexes, the minimum pulse width filter may introduce additional harmonic distortion which must be dealt with to comply with the grid codes.

In Table I the adaptive dc-link voltage reference output of the maximum modulation index controller is given for the power points considered in Figure 8 and 9. The operating junction temperatures of the IGBT and diode from the power modules are given in Table I where adaptive dc-link voltage was used, and in Table II without the use of adaptive control. The number of cycles to failure ($N_{c,f}$) is also calculated in both cases, for diode and IGBT, using the modified Coffin-Manson law presented in [10]. It can also be seen the reliability increase using the proposed method, by comparing the results from tables I and Table II.

Table I: Operating parameters using adaptive control

Adaptive							
Power [%]	V_{DC} [V]	$T_{j,max,IGBT}$	ΔT_{IGBT}	$T_{j,max,D}$	ΔT_D	$N_{c,f,IGBT}$	$N_{c,f,D}$
25 %	989	95	5.6	90	4.4	3.034e+28	5.134e+38
50 %	1001	108.5	10.9	95	6.3	2.969e+26	2.305e+36
75 %	1017	123.9	17	101.2	8.7	7.823e+24	8.084e+33
100 %	1037	142.2	24.3	107.3	11	2.648e+23	6.798e+31

Table II: Operating parameters without adaptive control

Non-Adaptive							
Power [%]	V_{DC} [V]	$T_{j,max,IGBT}$	ΔT_{IGBT}	$T_{j,max,D}$	ΔT_D	$N_{c,f,IGBT}$	$N_{c,f,D}$
25 %	1050	96.6	6.8	90.8	4.7	8.512e+27	2.022e+38
50 %	1050	109.3	11.2	96.1	6.7	2.414e+26	7.929e+35
75 %	1050	124.6	17.2	102.4	9.1	7.053e+24	3.027e+33
100 %	1050	142.6	24.5	107.9	11.3	2.436e+23	4.355e+31

Another factor that affects the reliability is the operating dc-link voltage. The higher the dc-link voltage, the higher is also the maximum electric field within the chosen power module. Due to high electric fields in power modules, it has been shown that another case of failure is due to cosmic radiation [11]. This has even higher impact when the power converter is placed at high altitude [12].

Experimental Results

To test the converter operation at different operating dc-link voltages, a test setup has been built. The principle schematic is shown in Figure 10, where power is circulating in single phase. A standard wind turbine power stack was used, see Figure 11, consisting of a three phase converter where one of the phases is not used. One leg produces the voltage that emulates the grid voltage, controlled in open loop, while the other leg controls the current in the inductor.

To measure the power loss for different operating points, a single phase power analyzer is measuring the dc-link voltage and current. The power modules used were Infineon FF1000R17 (1000 A, 1700 V), therefore the circulating current was limited to 598 A_{RMS}. The inductor value was 380 μH, with a series resistance of 3.2 $m\Omega$. The deadtime was set to 4 μs, and the minimum pulse width to 12 μs, for a 2.5 kHz switching frequency.

When using non-adaptive dc-link voltage control, the operating dc-link voltage was fixed at 1050 V. The AC parameters produced by the open loop phase leg were controlled at all operating points to 319 V_{RMS} (single phase system), 50 Hz. The closed loop control leg was controlling the current to the rated value 598 A and lower in relative steps of 25%.
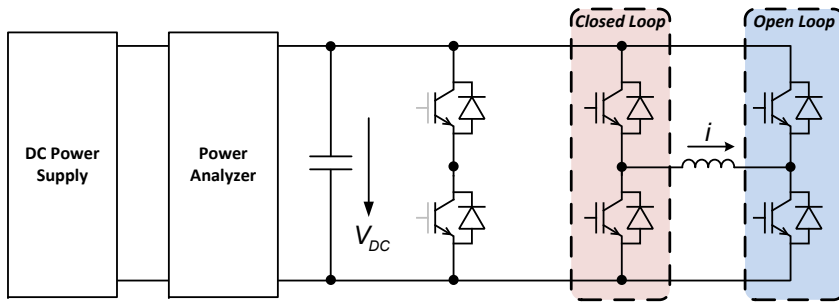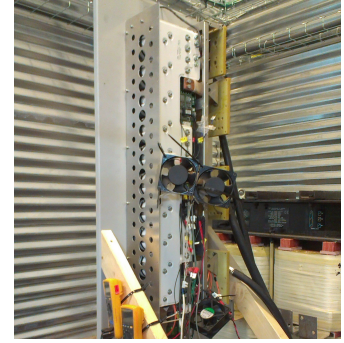
Figure 10: Test setup schematic

Figure 11: Test setup

The measured power loss in the previously described conditions are shown in Figure 12, and the scaled losses with respect to the non-adaptive test case are shown in Figure 13. The parameters used in the adaptive control are shown in Table III.
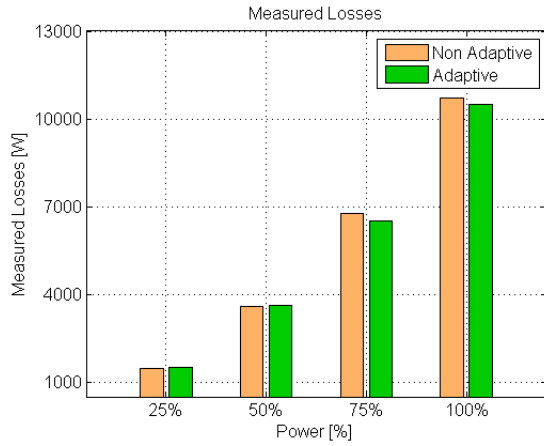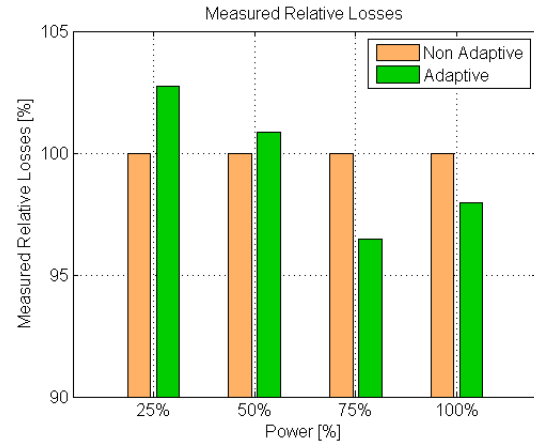

Figure 12: Measured losses

Figure 13: Measured relative losses

Table III: Operating parameters using adaptive control in experiments

Power [%]	i_{RMS} [A]	V_{DC} [V]	M_{max}
25 %	149.5	857	0.9867
50 %	299	910	0.9867
75 %	448.5	980	0.9867
100 %	598	1030	0.9867

In the presented experimental results, it can be noticed an increase in efficiency in the high power region (75 and 100 %). This directly reflects the reduction of the switching losses on the power semiconductor devices when using lower dc-link voltage. With a reduction of $20\,V$ the losses are reduced with more than 2% for the operation at rated power, as compared with the fixed voltage operation. At 75% of the rated power, the losses are reduced with more than 3.5%. For the lower power region however, it is noticed an increase of the power loss which is in contrast with the simulation results. The measured power loss however, includes the losses in power devices, dc-link capacitor but also the losses in the power inductor used to circulate the power. Therefore it is assumed that in the low power region, the additional losses are not present in the power semiconductors.

Conclusion

A controller that enhances the wind turbine converter performances was proposed. The dc-link voltage is adaptively controlled depending on the system state. The control is simple, implemented with a PI controller. The resulting operation is optimizing the dc-link voltage usage in the DC-AC power conversion. Simulation results proved that the efficiency and reliability can be increased and the grid current harmonic distortion slightly reduced. Additional gain in reliability is expected due to slightly reduced cosmic radiation influence, for lower dc-link operating voltage. Experimental results on a standard wind turbine power stack shows efficiency increase in the high power region. By reducing the operating dc-link voltage it is expected to increase the converter reliability due to reduced cosmic radiation failure.

References

[1] Blaabjerg, F.; Guerrero, J.M.; , "Smart grid and renewable energy systems," Electrical Machines and Systems (ICEMS), 2011 International Conference on , vol., no., pp.1-10, 20-23 Aug. 2011.

[2] Erlich, I.; Shewarega, F.; Feltes, C.; Koch, F.W.; Fortmann, J., "Offshore Wind Power Generation Technologies," Proceedings of the IEEE , vol.101, no.4, pp.891,905, April 2013

[3] Friedli, T.; Kolar, J.W.; Rodriguez, J.; Wheeler, P.W.; , "Comparative Evaluation of Three-Phase ACAC Matrix Converter and Voltage DC-Link Back-to-Back Converter Systems," Industrial Electronics, IEEE Transactions on , vol.59, no.12, pp.4487-4510, Dec. 2012.

[4] Dayaratne, U.I.; Tennakoon, S.B.; Shammas, N.Y.A.; Knight, J.S., "Investigation of variable DC link voltage operation of a PMSG based wind turbine with fully rated converters at steady state," Power Electronics and Applications (EPE 2011), Proceedings of the 2011-14th European Conference on , vol., no., pp.1,10, Aug. 30 2011-Sept. 1 2011.

[5] Hava, A.M.; Kerkman, R.J.; Lipo, T.A., "A high-performance generalized discontinuous PWM algorithm," Industry Applications, IEEE Transactions on , vol.34, no.5, pp.1059,1071, Sep/Oct 1998

[6] Liserre, M.; Dell'Aquila, A.; Blaabjerg, F.; , "Design and control of a three-phase active rectifier under non-ideal operating conditions," Industry Applications Conference, 2002. 37th IAS Annual Meeting. Conference Record of the , vol.2, no., pp.1181-1188 vol.2, 13-18 Oct. 2002.

[7] Teodorescu, R.; Liserre, M.; Rodriguez, P.;, "Grid converters for photovoltaic and wind power systems", vol. 29. Wiley, 2011.

[8] Blaabjerg, F.; Jaeger, U.; Munk-Nielsen, S.; , "Power losses in PWM-VSI inverter using NPT or PT IGBT devices," Power Electronics, IEEE Transactions on , vol.10, no.3, pp.358-367, May 1995.

[9] Schonberger, J.; , "Averaging methods for electrical-thermal converter models," Power Electronics and Applications (EPE 2011), Proceedings of the 2011-14th European Conference on , vol., no., pp.1-8, Aug. 30 2011-Sept. 1 2011.

[10] Scheuermann, U.; Hecht, U., "Power Cycling Lifetime of Advanced Power Modules for Different Temperature Swings", Proc. PCIM, PE4.5, 59-64, Nurnberg 2002.

[11] Kabza, H.; Schulze, H.-J.; Gerstenmaier, Y.; Voss, P.; Schmid, J.W.W.; Pfirsch, F.; Platzoder, K., "Cosmic radiation as a cause for power device failure and possible countermeasures," Power Semiconductor Devices and ICs, 1994. ISPSD '94., Proceedings of the 6th International Symposium on , vol., no., pp.9,12, 31 May-3 Jun 1994.

[12] Pfirsch, F.; Soelkner, G., "Simulation of cosmic ray failures rates using semiempirical models," Power Semiconductor Devices and IC's (ISPSD), 2010 22nd International Symposium on , vol., no., pp.125,128, 6-10 June 2010.